Spheromak Formation by Steady Inductive Helicity Injection

T. R. Jarboe, W. T. Hamp, R. Z. Aboul Hosn, G. J. Marklin, B. A. Nelson, R. G. O'Neill, A. J. Redd, P. E. Sieck, R. J. Smith, and J. S. Wrobel

University of Washington, Seattle, Washington

e-mail contact and main author: Jarboe@aa.washington.edu

Abstract. A spheromak is formed, for the first time, by a new steady state inductive helicity injection method. Using two inductive injectors with n = 1 symmetry and oscillating at 5.8 kHz, a steady state spheromak with n = 0 symmetry is formed and sustained through non-linear relaxation. A spheromak with about 12 kA of toroidal current is formed and sustained using about 3 MW of power. This is a much lower power threshold for spheromak production than required for electrode based helicity injection methods. Internal magnetic probe data, including oscillations driven by the injectors, agree with the plasma being in the Taylor state. The agreement is remarkable considering the only fitting parameter is the amplitude of the spheromak component of the state.

Magnetic helicity, the self-linkage of magnetic flux, is the best constant of motion for magnetized plasma in resistive magnetohydrodynamics. [1] Helicity is conserved on the time scales of energy dissipating instabilities and, on these time scales, magnetic configurations relax toward the state of Minimum Energy that Conserves Helicity (MECH state). [2] Only collisional resistive processes dissipate helicity. [3] Thus, to sustain a helicity containing magnetic structure for times longer than the resistive decay time, helicity must be injected. Since relaxation is on a shorter time scale than resistive decay, relaxation will maintain the configuration even if the helicity is injected with a different topology than that of the relaxed state. [4] Helicity injection, using coaxial electrodes (CHI), has been used to form and sustain spheromaks [5, 6, 7, 8] and spherical tori. [9, 10, 11, 12, 13] Helicity conservation has been confirmed experimentally. [14]

The spheromak is the minimum energy state for an oblate shaped spheroidal volume. [15] This equilibrium can have closed nested flux surfaces that should have good confinement with no material or coils linking the boundary. Thus, from an engineering point of view, it leads to a smaller much more cost effective reactor compared to configurations that have a toroidal vacuum vessel linked by large toroidal field coils.[16] With a boundary having a bowtie shaped cross section and helicity injection driving the edge, β-limits of 10% are possible. [17] However, the confinement must be sufficient so that the β-limit will be reached.

Decaying CHI produced spheromaks seem to have reasonable confinement. [18, 19] Ohmic heating to the β-limit has been achieved [20] and temperatures of several hundred electron volts have been reached. [21, 19] However, CHI sustained spheromaks have not achieved as impressive results. To eliminate electrodes and open field lines the helicity injected torus with steady inductive helicity injection (HIT-SI) has been built [22, 23, 24] to form and sustain a spheromak by Steady Inductive Helicity Injection (SIHI). This paper reports the first spheromak production and sustainment using SIHI in the HIT-SI experiment. The power required is only 3 MW, more than an order of magnitude lower than required for CHI spheromak production. [25]

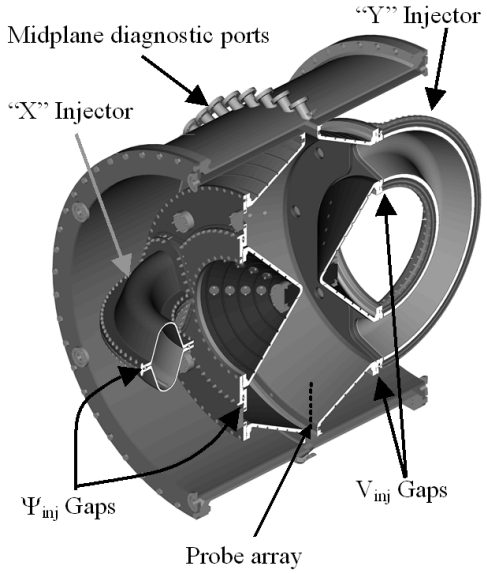

Figure 1. Crossection of the HIT-SI copper shell and insulating breaks used for steady inductive helicity injection. The locations of the magnetic probes of the probe array are shown. The toroidal grooves for the flux loops are shown.

Figure 1 shows a crossection of the HIT-SI device. The experiment has a bowtie shaped spheromak confinement region with two helicity injectors. The injectors are 180° segments of a small, elongated-crossection Reversed Field Pinch. In each injector the loop voltage and toroidal flux are oscillated in phase. The injectors are 90° out of phase with each other but have the same amplitude of voltage (V_o) and flux (ψ_o). This gives a constant helicity injection rate of $2V_o\psi_o$. [22] References 23 and 24 give a more detailed discussion of HIT-SI and its operation.

With flux boundary conditions the MECH state is the Taylor state and is found by solving $\nabla\times\mathbf{B} = \lambda\mathbf{B}$ inside the boundary where λ is a global constant. [26] In HIT-SI with no flux in the injectors, the Taylor state is a spheromak, having even symmetry, that is almost entirely axisymmetric ($n = 0$) with a small amount of $n = 2$ and the eigenvalue (λ_{sph}) is $10.4\ m^{-1}$. Adding toroidal flux in an injector allows any value of injector λ (λ_{inj}) to satisfy $\nabla\times\mathbf{B} = \lambda\mathbf{B}$ in the entire volume with odd symmetry. At small amounts of helicity, λ is less than λ_{sph} and the Taylor state has no spheromak current. As more helicity is added to the system, λ of this state increases until it reaches λ_{sph}. When the helicity is increased beyond this value the spheromak is formed and further increase in the system helicity leads to an increase in the spheromak fields without a change in λ. The geometry can hold an arbitrary amount of helicity with λ not exceeding λ_{sph}. Thus, when the helicity content is high enough to form a spheromak, the true Taylor state of HIT-SI is made up of three components: an odd component from each injector with their flux having just enough current so that λ_{inj} in each is equal λ_{sph}, and an even component, the spheromak, that has the strength needed to contain the remaining helicity. Figure 2a shows the magnetic field lines of the injector Taylor state when λ_{inj} equals λ_{sph}.

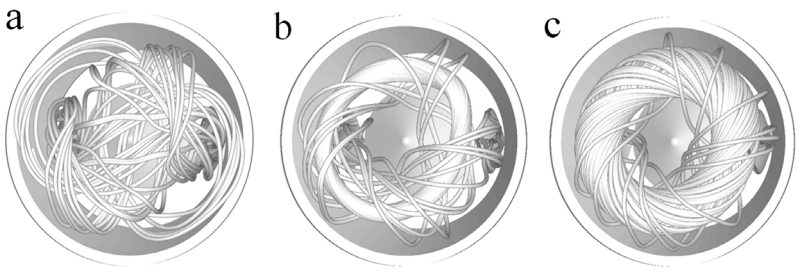

Figure 2. Magnetic fields of Taylor states with different amounts of spheromak current compared to the injector current. In a) the spheromak current is zero and the n=1 injector only Taylor state is shown. In b) the spheromak toroidal currents are 1.5 times that of the amplitude of the injectors. In c) the spheromak toroidal current is 5 times the injector amplitude. For all figures the phase is such that the shown injector is at the maximum current and flux and the other is at zero. All phases look qualitatively similar except, of course, for amount of flux that links each injector.

The superposition of Taylor states is still a Taylor state equilibrium if the λ is the same for all states in the superposition. The injectors have odd symmetry and solving $\nabla\times\mathbf{B} = \lambda\mathbf{B}$ with $\lambda = 10.4\ m^{-1}$ in the injectors does not couple to the even-symmetry spheromak. (In CHI, solving $\nabla\times\mathbf{B} = \lambda\mathbf{B}$ with $\lambda_{inj} = \lambda_{sph}$ gives infinite spheromak helicity because the injector and spheromak both have even symmetry.) Thus, by adding the spheromak state to the injector states, Taylor states with any ratio of injector current to spheromak current can be calculated. One important question is how much current the spheromak must have in order to have some closed flux field lines that do not link the injectors. Figure 2b shows the field lines of a Taylor state with the ratio approximately equal to that observed so far. Figure 2c shows what might be achieved with more optimization on HIT-SI. Figures b and c of Figure 2 have an isolated closed flux region that is surrounded by edge field lines that pass through the injectors. Thus, these Taylor states of HIT-SI have the proper topology for good plasma confinement. The threshold for this separatrix formation is about where the spheromak toroidal current is equal to the amplitude of the injector currents.

The measurement results given in this paper are from internal magnetic probes and flux loops external to the copper shell. (Both have at least 3% accuracy.) Figure 1 shows the location of the magnetic probe coils. The 20 flux loops are mounted in the toroidal groove in the outside surfaces of the flux conserver of the bow tie spheromak region, shown in Figure 1. Assuming the flux conserver is thin and the magnetic field is zero on the outside, the poloidal magnetic field on the inside can be calculated from the rate of flux loss and the surface resistance of the flux conserver. It is given by, $B_{pol} = (\mu_o\delta/2\pi R\eta)d\psi/dt$ where δ is the thickness of the flux conserver, R is the radius of the flux conserver, η is the resistivity of the flux conserver material, and ψ is the poloidal flux that has resistively diffused out of the flux conserver. The flux conserver is 12.7 mm thick chromium-copper with 80% the conductivity of pure copper. Figure 3 shows the injector parameters as a function of time during shot #104338. The voltage and flux are feedback controlled by pulse width modulation. The amplitude of the flux demand curve is a function of time in order to keep λ_{inj} as close as practical to $17\ m^{-1}$. The demand shape is determined from previous nearly identical shots. In practice λ_{inj} must be greater than λ_{sph} so there is free energy to drive relaxation. [27]

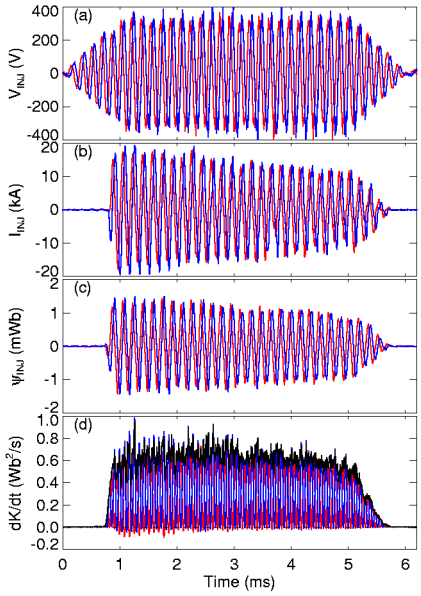

Figure 3. Injector parameters as a function of time; red for the X-injector and blue for the Y-injector. a) Loop voltage. b) Toroidal current. c) Toroidal flux. d) Helicity injection rate with black as the total of both injectors.

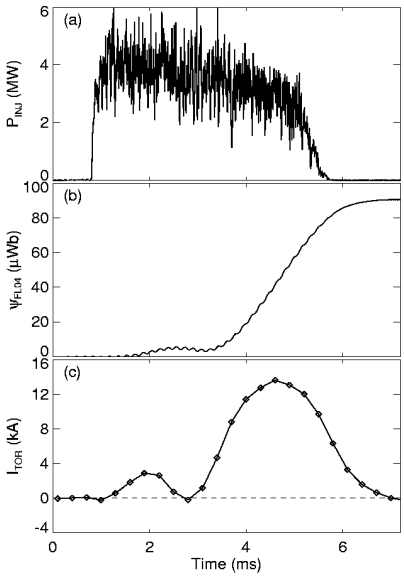

Figure 4. Spheromak parameters as a function of time. a) Total input power. b) Typical flux loss out of the shell as a function of time. c) Toroidal (n=0) spheromak current as a function of time.

Figure 4a shows the total power injected as a function of time. A flux loop signal is shown in Figure 4b, which gives a rate of loss of about 30 mWb/sec. Twenty such signals are used to find B_{pol} at the positions of the flux loops. Ampere's law is then used around the inside of the poloidal perimeter to calculate the toroidal current, assuming B_{pol} is equal to that measured by the nearest flux loop. Figure 4c shows the plasma current as a function of time. At its peak, the spheromak current is about 13.7 kA. A spheromak is formed only if both injectors inject the same sign of helicity; the flux and voltage are within 30^o of being in phase on both injectors; the power is above 2MW and the wall conditions are clean (base pressure low 10^{-8}torr). The direction of the spheromak current reverses when the rotation of the injector driven

structure is reversed. Figure 5 shows the toroidally averaged surface poloidal field on the flux conserver as deduced from the flux loop data, at the peak of the toroidal current. Also shown are the Taylor state values for the spheromak with the best least squares fit to the data, yielding 11.8 kA of toroidal spheromak current.

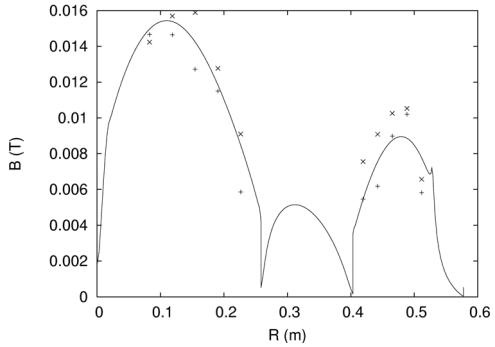

Figure 5. Plot of the poloidal magnetic field on the wall of the flux conserver as a function of the major radius. The data shown are from flux loop data. Data from the X-half of the flux conserver are shown with pluses (+) and data from the Y-half are shown with crosses (×). The solid curve is for the poloidal field at the wall of the Taylor-state spheromak.

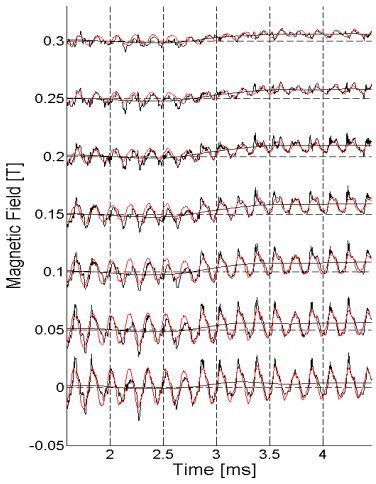

Figure 6a. Internal poloidal magnetic field for shot #104338 as a function of time. The Taylor state model predicts the red lines. From top to bottom the major radii of the probe positions are 0.514 m, 0.489 m, 0.464 m, 0.438 m, 0.413 m, 0.387 m, and 0.362 m. The traces are offset for clarity and the zero magnetic field value for each trace is at the nearest horizontal dashed line.

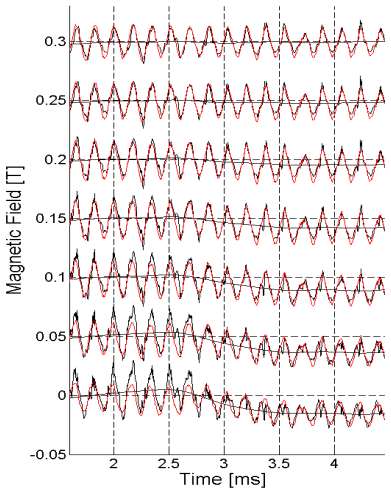

Figure 6b. Internal toroidal magnetic field for shot #104338 as a function of time. Presentation of data is the same as in Figure 6a.

Data from internal magnetic field probes are shown in Figure 6a and Figure 6b. The positions of the probes are shown in Figure 1. There are three overlaying traces at each position for poloidal and toroidal fields. The two black overlaying traces are the probe data with different low pass filters. One filter is at essentially the full bandwidth of the probe, 200 kHz. The other is heavily filtered at 1.5 kHz to eliminate most of the 5.8 kHz signal produced by the oscillating injectors, revealing the "steady state" component. Note that slightly before 3 ms a steady state component begins to grow. In the poloidal field, the steady state component at the wall exceeds the amplitude of the 5.8 kHz oscillation and the fields become unidirectional. For the toroidal field, the same behavior occurs but for the positions furthest from the wall.

The internal fields predicted by the model are also shown in Figure 6a and Figure 6b. The red traces are from the composite Taylor state that has the n = 0 spheromak λ (10.4 m^{-1}). The Taylor state with each injector having the measured injector current and the spheromak Taylor state are added to make the composite Taylor state. The amplitude of the spheromak state at 4.5 ms is found by doing a least squares fit to the steady state poloidal and toroidal fields at that time. This yields a spheromak state with a toroidal current of 12.3 kA for these data, which is about 123% of the injector current. See Figure 7 for this fit. For other times, these spheromak fields are multiplied by a scale factor equal to the toroidal field measured at R = 0.387 m divided by its value there at 4.5 ms. Thus, this method of fitting only assures fairly good agreement between the steady state values of the model and the experiment for the toroidal field data at R = 0.387 m. The agreement of the steady state values of all other traces depends on the accuracy of the Taylor state in representing the experiment.

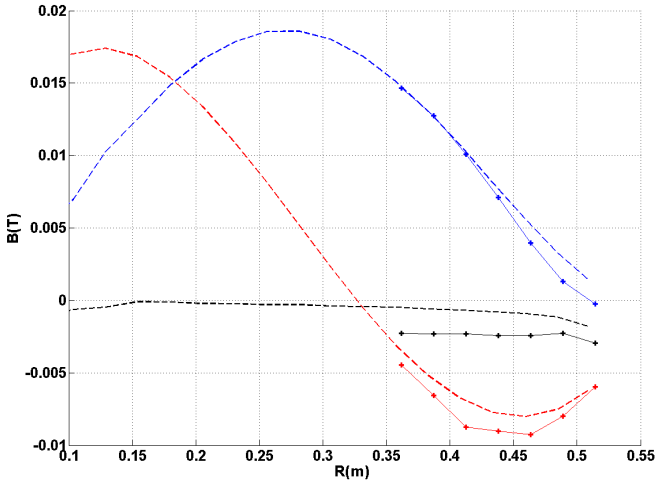

Figure 7. Least squares fit of the steady state probe data at 4.5 ms to the spheromak Taylor state. The blue curve shows the toroidal field data. The red and the black curves show the z-component and radial component of the poloidal field. The magnetic fields of the data and the Taylor state are plotted as a function of major radius. The dashed curves are the Taylor state values on the line defined by the probe array.

The model nearly matches the probe data and lets us understand the gross features of the equilibrium. It shows good agreement with the amplitude of the injector driven oscillations for all of the probe data. The phase of the oscillations is in fair agreement for both the toroidal field and the poloidal field. The steady state spheromak component agrees well with the toroidal field at all major radii, which may be due, in part, to forced agreement at R = 0.387 m. The poloidal data indicate that the magnetic axis has the same radius as the Taylor state. This is shown more clearly in Figure 7. These results clearly demonstrate that steady inductive helicity injection with n=1 symmetry can form and sustain a spheromak. The agreement with the Taylor model is remarkable and these initial results bode very well for this concept. The lifetime of the spheromak is not understood at this time, and it is not increased when the power is kept on for a longer time. While the density was not measured, similar discharges had FIR measure densities from a few to several times $10^{19}m^{-3}$. The electron temperature has not been measured on HIT-SI but similar spheromaks have had electron temperatures well under 100 eV. Ion Doppler spectroscopy (IDS) shows ion temperatures in the 10eV range, which is in the range expected for these low powers. The value of j/n is well below 10^{-14}Am so low-Z impurities have not burned through.

The Authors wish to thank Professor Masayoshi Nagata for the use of his IDS instrument and John Rogers, George Andexler, and Dan Lotz for their technical assistance. This work is sponsored by the United States Department of Energy.

References

[1] Edenstrasser J. W., Phys. Plasmas **2**, 1206 (1995).
[2] Taylor J. B., Rev. Mod. Phys. **58**, 741 (1986).
[3] Jarboe T. R., Plasma Phys. Control. Fusion **36**, 945 (1994).
[4] Fernández J. C. *et al.*, Phys. Fluids B, **1**, 1254 (1989).
[5] Jarboe T. R. *et al.*, Phys. Rev. Lett., **51**, 39 (1983)
[6] McLean H. S., Phys. Rev. Lett. **88**, 125004 (2002).
[7] Duck R. C. *et al.*, Plasma Phys. Control. Fusion, **39**, 715 (1997).
[8] al-Karkhy A. *et al*, Phys. Rev. Lett., **70**,1814 (1993).
[9] Jarboe T. R. *et al.*, Phys. Plasmas **5**, 1807 (1998).
[10] Nelson B. A. *et al.*, Phys. Plasmas **2**, 2337 (1995).
[11] Raman R. *et al*., Nuc. Fusion, **41,** 1081 (2001).
[12] Nagata, M. *et al*., Phys. Plasmas **10**, 2932 (2003).
[13] Gibson K. J. *et al.*, Plasma Phys. Control. Fusion **42,** 1331 (2000).
[14] Barnes C. W. *et al*., Phys. Fluids **29**, 3415 (1986).
[15] Rosenbluth M. N. and Bussac M. N., Nucl. Fusion, **19**, 489 (1979).
[16] Hagenson R. L. and Krakowski R. A., Fusion Technol. **8**, 1606 (1985).
[17] Shumlak U. and Jarboe T. R., Phys Plasmas, 7, 2959 (2000).
[18] Wysocki F. J. *et al*., Phys. Rev. Lett., **65**, 40 (1990).
[19] Wood D. R. *et al*., Nucl. Fusion **45**, 1582 (2005).
[20] Wysocki F. J. *et al*., Phys. Rev. Lett., **61**, 2457 (1988).
[21] Jarboe T. R. *et al.*, Phys. Fluids B, **2**, 1342 (1990).
[22] Jarboe, T. R., Fusion Technology, **36**, 85 (1999).
[23] Sieck P. E. *et al*., IEEE Trans. Plasma Sci., **33**, 723 (2005).
[24] Sieck P. E. *et al*., Nucl. Fusion **46,** 254 (2006).
[25] Barnes C. W. *et al*., Phys. Fluids. B **2**, 1871 (1990).
[26] Woltjer L., Proc. Natl. Acad. Sci. **44**, 489 (1958).
[27] Jarboe T. R. and Alper B., Phys. Fluids **30**, 1177 (1987).